logical Diseases and Mental Health, and for Comprehensive Research on Aging and Health from the Japanese Ministry of Health, Labour and Welfare, and by Grants-in-Aid for Young Scientists (B) and for Scientific Research (C) from the Japanese Ministry of Education, Culture, Sports, Science and Technology. We would like to thank Mr. Yusuke Urakubo, Mr. Yasutsugu Tsutsui, and Mr. Masashi Yoshimoto for their technical assistance.

References

Ahlskog, J.E., Muenter, M.D., 2001. Frequency of levodopa-related dyskinesias and motor fluctuations as estimated from the cumulative literature. Mov. Disord. 16, 448–458.

Asanuma, M., Miyazaki, I., Diaz-Corrales, F.J., Ogawa, N., 2004. Quinone formation as dopaminergic neuron-specific oxidative stress in pathogenesis of sporadic Parkinson's disease and neurotoxin-induced parkinsonism. Acta Med. Okayama 58, 221–233.

Asanuma, M., Miyazaki, I., Diaz-Corrales, F.J., Shimizu, M., Tanaka, K., Ogawa, N., 2005. Pramipexole has ameliorating effects on levodopa-induced abnormal dopamine turnover in parkinsonian striatum and quenching effects on dopamine-semiquinone generated *in vitro*. Neurol. Res. 27, 533–539.

Asanuma, M., Miyazaki, I., Ogawa, N., 2003. Dopamine- or L-DOPA-induced neurotoxicity: the role of dopamine quinone formation and tyrosinase in a model of Parkinson's disease. Neurotox. Res. 5, 165–176.

Basma, A.N., Morris, E.J., Nicklas, W.J., Geller, H.M., 1995. L-dopa cytotoxicity to PC12 cells in culture is via its autoxidation. J. Neurochem. 64, 825–832.

Chae, S.W., Bang, Y.J., Kim, K.M., Lee, K.Y., Kang, B.Y., Kim, E.M., Inoue, H., Hwang, O., Choi, H.J., 2007. Role of cyclooxygenase-2 in tetrahydrobiopterin-induced dopamine oxidation. Biochem. Biophys. Res. Commun. 359, 735–741.

Choi, H.J., Kim, S.W., Lee, S.Y., Hwang, O., 2003. Dopamine-dependent cytotoxicity of tetrahydrobiopterin: a possible mechanism for selective neurodegeneration in Parkinson's disease. J. Neurochem. 86, 143–152.

Choi, H.J., Lee, S.Y., Cho, Y., Hwang, O., 2005. Inhibition of vesicular monoamine transporter enhances vulnerability of dopaminergic cells: relevance to Parkinson's disease. Neurochem. Int. 46, 329–335.

Foppoli, C., Coccia, R., Cini, C., Rosei, M.A., 1997. Catecholamines oxidation by xanthine oxidase. Biochim. Biophys. Acta 1334, 200–206.

Fornstedt, B., Rosengren, E., Carlsson, A., 1986. Occurrence and distribution of 5-*S*-cysteinyl derivatives of dopamine, dopa and dopac in the brains of eight mammalian species. Neuropharmacology 25, 451–454.

Gerlach, M., Double, K.L., Ben-Shachar, D., Zecca, L., Youdim, M.B., Riederer, P., 2003. Neuromelanin and its interaction with iron as a potential risk factor for dopaminergic neurodegeneration underlying Parkinson's disease. Neurotox. Res. 5, 35–44.

Graham, D.G., 1978. Oxidative pathways for catecholamines in the genesis of neuromelanin and cytotoxic quinones. Mol. Pharmacol. 14, 633–643.

Haque, M.E., Asanuma, M., Higashi, Y., Miyazaki, I., Tanaka, K., Ogawa, N., 2003. Apoptosis-inducing neurotoxicity of dopamine and its metabolites via reactive quinone generation in neuroblastoma cells. Biochim. Biophys. Acta 1619, 39–52.

Hastings, T.G., 1995. Enzymatic oxidation of dopamine: the role of prostaglandin H synthase. J. Neurochem. 64, 919–924.

Hastings, T.G., Lewis, D.A., Zigmond, M.J., 1996. Role of oxidation in the neurotoxic effects of intrastriatal dopamine injections. Proc. Natl. Acad. Sci. U.S.A. 93, 1956–1961.

Kito, M., Maehara, M., Watanabe, K., 1996. Mechanisms of T-type calcium channel blockade by zonisamide. Seizure 5, 115–119.

Komatsu, M., Hiramatsu, M., Willmore, L.J., 2000. Zonisamide reduces the increase in 8-hydroxy-2'-deoxyguanosine levels formed during iron-induced epileptogenesis in the brains of rats. Epilepsia 41, 1091–1094.

Korytowski, W., Sarna, T., Kalyanaraman, B., Sealy, R.C., 1987. Tyrosinase-catalyzed oxidation of dopa and related catechol(amine)s: a kinetic electron spin resonance investigation using spin-stabilization and spin label oximetry. Biochim. Biophys. Acta 924, 383–392.

Kuhn, D.M., Arthur Jr., R.E., Thomas, D.M., Elferink, L.A., 1999. Tyrosine hydroxylase is inactivated by catechol-quinones and converted to a redox-cycling quinoprotein: possible relevance to Parkinson's disease. J. Neurochem. 73, 1309–1317.

Lai, C.T., Yu, P.H., 1997. Dopamine- and L-β-3,4-dihydroxyphenylalanine hydrochloride (L-Dopa)-induced cytotoxicity towards catecholaminergic neuroblastoma SH-SY5Y cells. Effects of oxidative stress and antioxidative factors. Biochem. Pharmacol. 53, 363–372.

LaVoie, M.J., Ostaszewski, B.L., Weihofen, A., Schlossmacher, M.G., Selkoe, D.J., 2005. Dopamine covalently modifies and functionally inactivates parkin. Nat. Med. 11, 1214–1221.

Machida, Y., Chiba, T., Takayanagi, A., Tanaka, Y., Asanuma, M., Ogawa, N., Koyama, A., Iwatsubo, T., Ito, S., Jansen, P.H., Shimizu, N., Tanaka, K., Mizuno, Y., Hattori, N., 2005. Common anti-apoptotic roles of parkin and alpha-synuclein in human dopaminergic cells. Biochem. Biophys. Res. Commun. 332, 233–240.

Miyazaki, I., Asanuma, M., Diaz-Corrales, F.J., Fukuda, M., Kitaichi, K., Miyoshi, K., Ogawa, N., 2006. Methamphetamine-induced dopaminergic neurotoxicity is regulated by quinone formation-related molecules. FASEB J. 20, 571–573.

Miyazaki, I., Asanuma, M., Diaz-Corrales, F.J., Miyoshi, K., Ogawa, N., 2005. Dopamine agonist pergolide prevents levodopa-induced quinoprotein formation in parkinsonian striatum and shows quenching effects on dopamine-semiquinone generated *in vitro*. Clin. Neuropharmacol. 28, 155–160.

Mori, A., Noda, Y., Packer, L., 1998. The anticonvulsant zonisamide scavenges free radicals. Epilepsy Res. 30, 153–158.

Murata, M., 2004. Novel therapeutic effects of the anti-convulsant, zonisamide, on Parkinson's disease. Curr. Pharm. Des. 10, 687–693.

Murata, M., et al., 2007. Zonisamide improves motor function in Parkinson disease: a randomized, double-blind study. Neurology 68, 45–50.

Murata, M., Horiuchi, E., Kanazawa, I., 2001. Zonisamide has beneficial effects on Parkinson's disease patients. Neurosci. Res. 41, 397–399.

Offen, D., Ziv, I., Sternin, H., Melamed, E., Hochman, A., 1996. Prevention of dopamine-induced cell death by thiol antioxidants: possible implications for treatment of Parkinson's disease. Exp. Neurol. 141, 32–39.

Ogawa, N., Asanuma, M., Miyazaki, I., Diaz-Corrales, F.J., Miyoshi, K., 2005. L-DOPA treatment from the viewpoint of neuroprotection: possible mechanism of specific and progressive dopaminergic neuronal death in Parkinson's disease. J. Neurol. 252 (Suppl. 4), iv23–iv31.

Ogawa, N., Edamatsu, R., Mizukawa, K., Asanuma, M., Kohno, M., Mori, A., 1993. Degeneration of dopaminergic neurons and free radicals. Possible participation of levodopa. Adv. Neurol. 60, 242–250.

Ogawa, N., Tanaka, K., Asanuma, M., 2000. Bromocriptine markedly suppress levodopa-induced abnormal increase of dopamine turnover in the parkinsonian striatum. Neurochem. Res. 25, 755–758.

Okada, M., Kaneko, S., Hirano, T., Ishida, M., Kondo, T., Otani, K., Fukushima, Y., 1992. Effects of zonisamide on extracellular levels of monoamine and its metabolite, and on Ca^{2+} dependent dopamine release. Epilepsy Res. 13, 113–119.

Okada, M., Kaneko, S., Hirano, T., Mizuno, K., Kondo, T., Otani, K., Fukushima, Y., 1995. Effects of zonisamide on dopaminergic system. Epilepsy Res. 22, 193–205.

Paz, M.A., Fluckiger, R., Boak, A., Kagan, H.M., Gallop, P.M., 1991. Specific detection of quinoproteins by redox-cycling staining. J. Biol. Chem. 266, 689–692.

Rosei, M.A., Blarzino, C., Foppoli, C., Mosca, L., Coccia, R., 1994. Lipoxygenase-catalyzed oxidation of catecholamines. Biochem. Biophys. Res. Commun. 200, 344–350.

Sulzer, D., Bogulavsky, J., Larsen, K.E., Behr, G., Karatekin, E., Kleinman, M.H., Turro, N., Krantz, D., Edwards, R.H., Greene, L.A., Zecca, L., 2000. Neuromelanin biosynthesis is driven by excess cytosolic catecholamines not accumulated by synaptic vesicles. Proc. Natl. Acad. Sci. U.S.A. 97, 11869–11874.

Sulzer, D., Zecca, L., 2000. Intraneuronal dopamine-quinone synthesis: a review. Neurotox. Res. 1, 181–195.

Suzuki, S., Kawakami, K., Nishimura, S., Watanabe, Y., Yagi, K., Seino, M., Miyamoto, K., 1992. Zonisamide blocks T-type calcium channel in cultured neurons of rat cerebral cortex. Epilepsy Res. 12, 21–27.

Tse, D.C., McCreery, R.L., Adams, R.N., 1976. Potential oxidative pathways of brain catecholamines. J. Med. Chem. 19, 37–40.

Walkinshaw, G., Waters, C.M., 1995. Induction of apoptosis in catecholaminergic PC12 cells by L-DOPA. Implications for the treatment of Parkinson's disease. J. Clin. Invest. 95, 2458–2464.

Whitehead, R.E., Ferrer, J.V., Javitch, J.A., Justice, J.B., 2001. Reaction of oxidized dopamine with endogenous cysteine residues in the human dopamine transporter. J. Neurochem. 76, 1242–1251.

Xu, Y., Stokes, A.H., Roskoski Jr., R., Vrana, K.E., 1998. Dopamine, in the presence of tyrosinase, covalently modifies and inactivates tyrosine hydroxylase. J. Neurosci. Res. 54, 691–697.

Zecca, L., Zucca, F.A., Wilms, H., Sulzer, D., 2003. Neuromelanin of the substantia nigra: a neuronal black hole with protective and toxic characteristics. Trends Neurosci. 26, 578–580.

Magn Reson Med Sci, Vol. 7, No. 3, pp. 163-167, 2008

CASE REPORT

Diffusion Tensor Imaging in Familial Spastic Paraplegia with Mental Impairment and Thin Corpus Callosum

Miho OTA[1], Noriko SATO[1]*, Yuji SAITOH[2], Fumito ENDO[2], Miho MURATA[2], and Takashi ASADA[3]

Departments of [1]Radiology and [2]Neurology, National Center Hospital for Mental, Nervous and Muscular Disorders, National Center of Neurology and Psychiatry
4-1-1, Ogawahigashi, Kodaira, Tokyo 187-8551, Japan
[3]Department of Neuropsychiatry, Institute of Clinical Medicine, University of Tsukuba
(Received April 17, 2008; Accepted July 2, 2008)

We investigated 2 Japanese siblings with a complicated form of familial spastic paraplegia. Cranial magnetic resonance (MR) imaging revealed marked thinning of the corpus callosum. Diffusion tensor imaging (DTI) showed microstructural changes in the thalamus, basal ganglia, and cerebral white matter, and single photon emission computed tomography (SPECT) using 99mTc-ethylcysteinate dimer showed very similar findings. DTI and SPECT effectively revealed global changes not revealed by conventional MR imaging.

Keywords: ***diffusion tensor imaging, familial spastic paraplegia, fractional anisotropy, mean diffusivity***

Introduction

Familial spastic paraplegia (FSP) is clinically and genetically heterogenous. It has been clinically classified into 2 categories, pure spastic paraplegia (pure FSP) and a "complicated" form.[1] In addition to spastic paraplegia, complicated FSP is associated with various somatic abnormalities and neurological deficits, including optic neuropathy, retinopathy, pyramidal symptom, neural amyotrophy, mental impairment, and cerebellar deficit.[1,2]

We report 2 patients with complicated FSP whose unique complications include mental deterioration and thin corpus callosum (CC) on magnetic resonance (MR) imaging. We examined diffusion tensor imaging (DTI) studies of the 2 patients with FSP and normal controls. We also performed single photon emission computed tomography (SPECT) using 99mTc-ethylcysteinate dimer (99mTc-ECD) on the patients.

Case Report

We examined 2 brothers (Patient 1, aged 27 years; Patient 2, 17 years) in a Japanese nuclear family, both of whom were clearly affected by familial spastic paraplegia (FSP) and were admitted to our hospital with progressive gait disturbance that began in their teens and became spastic. Psychomotor development was almost normal. Neurological examination revealed pyramidal signs in the upper and lower limbs in Patient 1 and limited to the lower limbs in Patient 2. No cataracts, retinal degeneration, or cerebellar dysfunction were evident. Patient 1 showed amyotrophy of the upper and lower limbs and trunk, loss of vibratory sensation in the lower limbs, and bladder dysfunction. Patient 2 only exhibited weakness in his lower legs. Evaluation using the Wechsler Adult Intelligence Scale-Revised demonstrated intellectual decline (intelligence quotient [IQ]: Patient 1, 41; Patient 2, 64). Serum vitamin B_{12}, thyroid function, and plasma very-long-chain fatty acid levels were normal. Serum was negative for antihuman T-cell lymphotrophic virus type-1 antibody.

Their father exhibited gait disturbance during his teens but showed no other neurological disturbance or mental deterioration. Their mother was free from degenerative neurological disorders. No other family member of the patients' or their parents' generation appeared to be affected by FSP.

The 2 siblings and 8 normal male controls (mean age = 27.8 ± 1.0 year) underwent magnetic resonance (MR) imaging; only the 2 siblings underwent single photon emission computed tomography

*Corresponding author, Phone: +81-42-341-2711, Fax: +81-42-346-2094, E-mail: snoriko@ncnp.go.jp

(SPECT). We explained the nature and purpose of the diffusion tensor imaging (DTI), MR imaging, and SPECT examinations and received the patients' informed consent. The protocol was approved by the local ethics committee. A complete description of our method was reported previously.[3,4] We performed MR imaging using a 1.0T unit (Magnetom Harmony; Siemens, Erlangen, Germany) with a head coil. Three-dimensional (3D) T_1-weighted images were scanned in the sagittal plane (repetition time/echo time [TR/TE], 2080/3.93 ms; flip angle, 15°; effective section thickness, 1.23 mm; slab thickness, 177 mm; matrix, 208×256; field of view [FOV], 256×315 mm; number of signals acquired, 1), yielding 144 contiguous slices through the head. In addition to 3D T_1-weighted images, we acquired conventional axial T_2-weighted turbo spin echo images (6580/89; slice thickness, 5 mm; intersection gap, 0.4 mm; matrix, 512×532; field of view, 230×230 mm; number of signals acquired, 1). DTI was performed in the axial plane (TE, 113 ms; TR, 10,100 ms; FOV, 230×230 mm^2; matrix, 128×128; 40 continuous transverse slices; slice thickness 3 mm with no intersection gap). To enhance signal-to-noise ratio, we repeated acquisition 5 times. We measured diffusion along 12 non-collinear directions using a diffusion-weighted b factor in each direction of 700 s/mm^2, and we acquired one image without using a diffusion gradient. We performed SPECT of the brain using 3-head rotation gamma cameras (MultiSPECT3; Siemens Medical System, Inc., Hoffman Estate, IL) equipped with high-resolution fan-beam collimators with 600 MBq of 99mTc-ECD. For each camera, projection data were obtained in a 128×128 format for 24 angles at 50 s per angle. A Shepp and Logan Hanning filter was used for SPECT image reconstruction at 0.7 cycle/cm. Attenuation correction was performed using Chang's method.

In Patient 1, T_1- and T_2-weighted cranial MR imaging showed extreme thinning of the CC and atrophy of the frontal, temporal, and parietal cortices (Fig. 1A, B, C). T_2-weighted images showed subtle high intensity in the frontal and parietal white matter (Fig. 1C). In Patient 2, images showed only severe thinning of the CC (Fig. 2A), particularly in the anterior half. No atrophy or abnormal signals were indicated in the cerebral hemispheres, cerebellum, or brainstem, with the exception of mild enlargement of the left trigone of the lateral ventricle (Fig. 2A, B, C). We investigated the regional callosal size, genu, splenium, and body. The corpus callosum was manually traced on the midsagittal slice of the T_1- weighted MR image. In Patient 1, the size of the genu was 28.7 mm^2; body, 86.2 mm^2; and splenium, 43.9 mm^2, In Patient 2, the size of the genu was 16.6 mm^2; body, 99.9 mm^2; and splenium, 96.8 mm^2. In controls, the mean sizes were: genu, 153.9 ± 19.0 mm^2; body, 318.8 ± 39.5 mm^2; and splenium, 83.1 ± 30.3 mm^2.

In Patient 1, 99mTc-ECD SPECT images showed diffuse decrease of blood flow in the cerebral cortex as well as both thalami and the left putamen (Fig. 1D). In Patient 2, SPECT images showed hypoperfusion in the left occipital cortex, both frontal cortices and thalami, and the left striatum (Fig. 2D).

We used the normalization method to investigate the differences of DTI metrics between the patients with FSP and healthy subjects. At normalization, the individual 3D T_1 image was first aligned to its b=0 image using statistical parametric mapping (SPM2) (Wellcome Department of Imaging Neuroscience, London, UK), and the aligned T_1 image was normalized to the standard Montreal Neurological Institute space, then the transformation matrix was applied to the fractional anisotropy (FA) and mean diffusivity (MD). Further, to avoid the effect of cerebrospinal fluid (CSF) diffusivity, FA and MD map images were masked with the CSF image derived from the segmented 3D T_1 image using SPM2. Then, each map was spatially smoothed by 5-mm full-width at half the maximum Gaussian. Statistical analyses were performed using SPM2 software. Decrease of FA and increase of MD in the cerebrums of patients with FSP compared to controls were evaluated using 2-sample T-test. Only differences meeting these criteria were deemed statistically significant. In this case, a seed level of $P<0.001$ (uncorrected) and a cluster level of $P<0.05$ (uncorrected) were selected.

The FA and MD values showed significant differences between patients and controls (FA; Figs. 1 E-H and 2 E-H; MD: Figs. 1 I-L and 2 I-L). The DTI metrics, especially the MD values of patients were significantly changed in the thalamus, basal nuclei except for the caudate, and almost entire cerebral white matter in Patient 1. In Patient 2, the decrease of FA value was not obviously detected in thalami and basal nuclei, but MD values were clearly increased as in Patient 1.

Discussion

Complicated FSP is associated with slowly progressive spastic paraplegia of juvenile onset, probably autosomal recessive type inheritance, moderate-to-severe mental impairment, and often, markedly thin corpus callosum. Our patients had quite analogous manifestations and presented similar

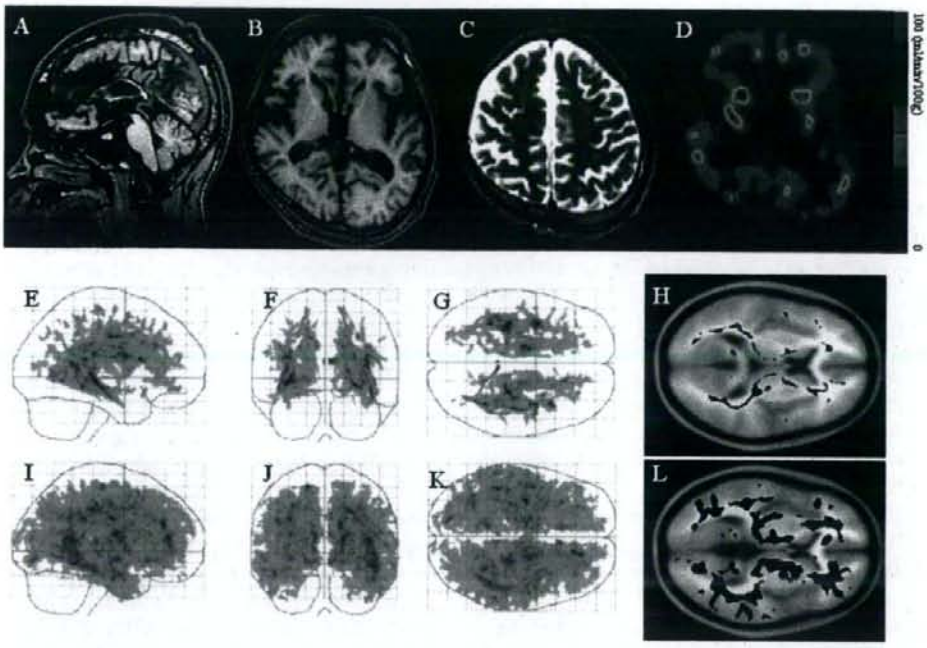

Fig. 1. Patient 1, a 27-year-old man with familial spastic paraplegia. **A**: Sagittal T_1-weighted image shows extremely thin corpus callosum (CC). **B**: Axial T_1-weighted magnetic resonance (MR) image shows frontal, temporal cortical atrophy. The trigones of the lateral ventricle are dilated. **C**: Axial T_2-weighted MR image shows subtle high intensity in the atrophic frontal and parietal white matter. **D**: Single photon emission computed tomography (SPECT) image shows diffuse decrease in blood flow in the cerebral cortex as well as both thalami and the left putamen. **E-H**: The decreased region of fractional anisotropy (FA) value depicted on the standard normalized space (2-sample t-test, statistical parametric mapping [SPM] 2). Significantly low FA values were detected in the thalamus and almost the entire cerebral white matter. **I-L**: The increased region of mean diffusivity (MD) value is shown. Similar to FA study, significantly high MD is revealed.

imaging findings to those of previously reported patients with FSP.[5-7] CC thinning, a characteristic finding, could have resulted from atrophy or hypoplasia.[5-9] However, Nakamura showed that CC thickness did not correlate with duration from onset, and they showed no change on MR imaging in a 5-year follow-up study.[6] Hence, hypoplasia appears the most likely mechanism of CC thinning. Although previous studies discussed causality of hypoplasia, little is known about its origin.[6,7]

Both patients showed global degeneration of white matter. In particular, degeneration of the thalami has been thought to contribute to intellectual decline in patients with FSP,[7] and our results showed high MD in the thalami in both patients, findings consistent with previous postmortem and neuroimaging study.[5,7,9,10] There are thalamic regions with only weak or diffuse cortical connections. Some connections obscured the directionality of diffusion, and the FA map detected no thalamic changes. Additionally, the statistical power of FA was relatively low. Because spatial normalization of subcortical white matter is less effective,[11] the more heterogeneous FA map rather than the relatively uniform MD map cannot be normalized well.[12] So, we could not reveal global white matter change so clearly from statistics using FA than using MD in this study. We could not detect the changes in the CC by DTI analysis but obtained other parts of cerebral FA and MD maps in patients with FSP. Because the abnormal thin structural change of CC and widened lateral cerebral ventricles in patients with FSP influenced the SPM segmentation of 3D-T_1 images, the masking process of the DTI map was ineffective.

DTI revealed diffuse microstructural changes of the white matter not detected by conventional MR imaging. In Patient 2, these changes preceded cortical change. The changes in regional cerebral blood flow revealed by 99mTc-ECD SPECT also preced-

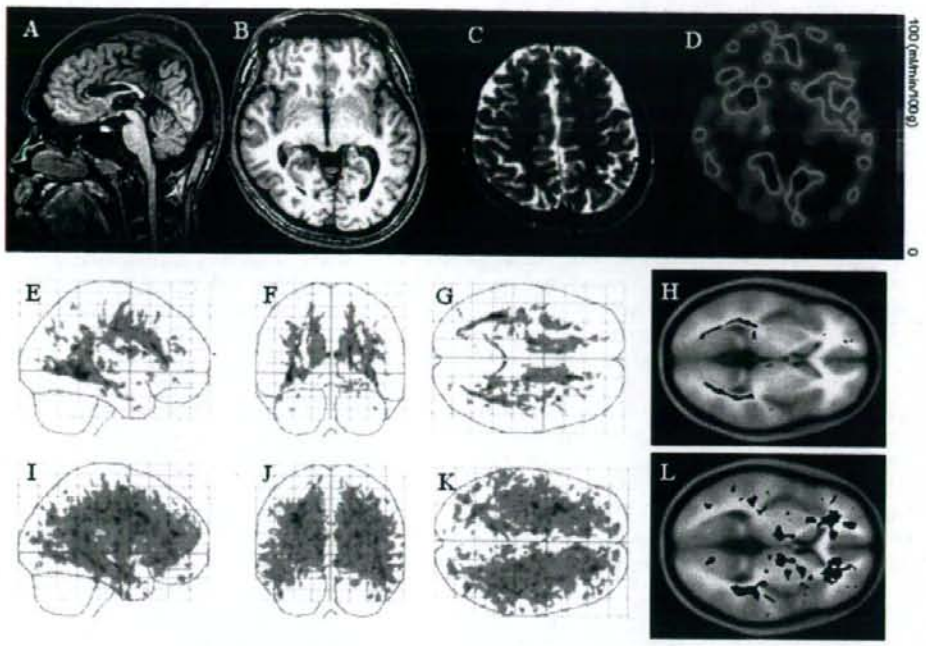

Fig. 2. Patient 2, 17-year-old younger brother with familial spastic paraplegia. **A**: Sagittal T_1-weighted image showing thin corpus callosum (CC), particularly in the anterior half. **B**: Axial T_1-weighted MR image shows relatively preserved cortex. The trigone of the left lateral ventricle is slightly dilated. **C**: Axial T_2-weighted magnetic resonance (MR) image shows no abnormal signals. **D**: Single photon emission computed tomography (SPECT) image shows hypoperfusion in the left occipital cortex, both frontal cortices and thalami, and the left striatum. **E-H**: The decreased region of fractional anisotropy (FA) value depicted on the standard normalized space (2-sample t-test, statistical parametric mapping [SPM] 2). Significantly low FA value was detected in the entire cerebral white matter, especially the optic radiations. **I-L**: The increased region of MD value is shown. Significantly high MD was revealed, similar to the findings in Patient 1.

ed structural changes measured by conventional MR imaging. The present SPECT findings showed relative preservation of the caudate blood flow, which was consistent with DTI findings. Previous study investigating FSP using MR spectroscopy and DTI indicated that the primary pathophysiological process in FSP affects the axon, possibly as a result of impaired axonal trafficking.[10] The same pattern of DTI metrics and cerebral blood flow changes reported here may be attributed to this pathophysiological process.

Conclusion

DTI revealed microstructural global changes of the white matter well, and such changes predate cortical deterioration. Changes in regional cerebral blood flow also preceded changes measured by conventional MR imaging, and DTI by MR and SPECT equally showed early pathophysiological process in FSP. Furthermore, DTI does not expose patients to radiation and is cost effective. We therefore recommend noninvasive DTI as equivalent to SPECT for evaluating intracranial morphometric changes in patients affected by FSP.

References

1. Harding AE. Complicated forms of hereditary spastic paraplegia, In: Harding AE, eds. The hereditary ataxias and related disorders. London: Churchill Livingstone, 1984; 191–204.
2. Sutherland JM. Familial spastic paraplegia, In: Vinken PJ, Bruyn GW, eds. Handbook of clinical neurology, vol. 22. Amsterdam: North-Holland, 1975; 421–431.
3. Hirao K, Ohnishi T, Hirata Y, et al. The prediction of rapid conversion to Alzheimer's disease in mild cognitive impairment using regional cerebral blood flow SPECT. Neuroimage 2005; 28:1014–1021.

4. Ota M, Sato N, Ohya Y, et al. Relationship between diffusion tensor imaging and brain morphology in patients with myotonic dystrophy. Neurosci Lett 2006; 407:234–239.
5. Iwabuchi K, Yagishita S, Amano N, Kosaka K. [A new type of complicated form of hereditary spastic paraplegia showing mental deterioration, quadriplegia with muscular atrophy, sensory disturbance, extrapyramidal disorders, and epilepsy.] Rinsho Shinkeigaku 1991; 31:945–952. Article in Japanese.
6. Nakamura A, Izumi K, Umehara F, et al. Familial spastic paraplegia with mental impairment and thin corpus callosum. J Neurol Sci 1995; 131:35–42.
7. Ueda M, Katayama Y, Kamiya T, et al. Hereditary spastic paraplegia with a thin corpus callosum and thalamic involvement in Japan. Neurology 1998; 51:1751–1754.
8. Yamashita I, Sasaki H, Yabe I, et al. Recessively inherited spastic paraplegia associated with ataxia, congenital cataracts, thin corpus callosum and axonal neuropathy. Acta Neurol Scand 2000; 102:65–69.
9. Ferrer I, Olivé M, Rivera R, Pou A, Narberhaus B, Ugarte A. Hereditary spastic paraparesis with dementia, amyotrophy and peripheral neuropathy. A neuropathological study. Neuropathol Appl Neurobiol 1995; 21:255–261.
10. Dreha-Kulaczewski S, Dechent P, Helms G, Frahm J, Gärtner J, Brockman K. Cerebral metabolic and structural alterations in hereditary spastic paraplegia with thin corpus callosum assessed by MRS and DTI. Neuroradiology 2006; 48:893–898.
11. Eriksson SH, Rugg-Gunn FJ, Symms MR, Barker GJ, Duncan JS. Diffusion tensor imaging in patients with epilepsy and malformations of cortical development. Brain 2001; 124:617–626.
12. Snook L, Plewes C, Beaulieu C. Voxel based versus region of interest analysis in diffusion tensor imaging of neurodevelopment. Neuroimage 2007; 34:243–252.

Treatment of neuromyelitis optica: Current debate

Therapeutic Advances in Neurological Disorders
[2008] 1(1) 43–52
DOI: 10.1177/1756285608093978

Tomoko Okamoto, Masafumi Ogawa, Youwei Lin, Miho Murata, Sachiko Miyake and Takashi Yamamura

***Abstract*:** Neuromyelitis optica (NMO) is an inflammatory demyelinating disease that largely affects optic nerves and spinal cord. Recent studies have identified an elevation of serum anti-aquaporin 4 antibody as a hallmark of NMO. Typical cases of NMO significantly differ from multiple sclerosis (MS) in immunological markers, histopathology, and responses to therapy. In fact, plasma exchange may be more efficacious for NMO than MS, whereas interferon-β is recommended for MS but not for NMO. An emerging idea that pathogenesis of NMO may involve an interaction of the newly identified helper T cell subset, Th17, with B cells offers potential targets of therapy.

***Keywords*:** neuromyelitis optica, multiple sclerosis, Th17 cells, anti-aquaporin-4 antibody, interferon-β

Introduction

Neuromyelitis optica (NMO; Devic syndrome) is an inflammatory disease of the central nervous system (CNS) that affects optic nerves and spinal cord [Jacob *et al.* 2007; Matiello *et al.* 2007; Wingerchuk *et al.* 2007]. In older literature, NMO was defined as a disorder that is characterized by development of a single episode of bilateral optic neuritis and transverse myelitis (Table 1). However, recent studies have indicated that presence of serum antibodies against aquaporin 4 (AQP4), a water channel protein, is a hallmark of NMO and could be essential for making the diagnosis. Since anti-AQP4 antibody became recognised as a serological marker of NMO, the clinical picture of NMO has been significantly broadened. Indeed, when the latest criteria [Wingerchuk *et al.* 2006] are used for diagnosis of NMO, a large majority of the NMO patients follow a relapsing clinical course and sometimes develop brain lesions.

Of interest, NMO has been traditionally separated from multiple sclerosis (MS) in western countries, whereas they have been integrated into the category of MS in Japan, by giving a term 'opticospinal MS (OSMS)'. Because not all OSMS exhibit an elevation of anti-AQP4 antibody titer in the sera, and because OSMS may develop brain lesions characteristic of MS [Barkhof *et al.* 1997], it is still debatable as to whether OSMS and NMO may cover an entirely identical disease spectrum or not.

Nowadays, a large proportion of patients with MS are being treated with standard drugs such as interferon-β and glatiramer acetate. It has been reported that interferon-β may also be efficacious for NMO/OSMS based on analysis of a small number of patients [Saida *et al.* 2005]. However, more recent works have emphasized the differences in immunological and pathological features between NMO and conventional MS, which indicates the relevance of distinctive therapeutic strategies for NMO and MS. The aim of this review is to provide up-dated information on the diagnosis and treatment of NMO and also discuss the immunological pathogenesis of NMO with special reference to a critical interaction between B cells and Th17 cells, a newly identified helper T cell subset [Hsu *et al.* 2008].

Diagnosis of NMO: discovery of anti-aquaporin 4 (AQP4) antibody and its impact

In general, the clinical picture of typical NMO is very different from that of conventional MS. Important points for differential diagnosis are as

Correspondence to:
Takashi Yamamura
Department of Neurology, National Center Hospital of Neurology and Psychiatry, Kodaira, Tokyo, Japan
Department of Immunology, National Institute of Neuroscience, National Center of Neurology and Psychiatry, Kodaira, Tokyo, Japan
yamamura@ncnp.go.jp

Tomoko Okamoto
Masafumi Ogawa
Youwei Lin
Miho Murata
Department of Neurology, Musashi Hospital, National Center of Neurology and Psychiatry, Kodaira, Tokyo, Japan

Youwei Lin
Sachiko Miyake
Department of Immunology, National Institute of Neuroscience, National Center of Neurology and Psychiatry, Kodaira, Tokyo, Japan

follows: (1) Optic neuritis in NMO could be much more serious than in MS, and often leads to blindness, (2) MRI scan of NMO often reveals presence of an extensive lesion extending over three vertebral segments (Figure 1), referred to as 'Longitudinally extensive spinal cord lesion' (LESL), (3) Oligoclonal bands (OBs) commonly found in the cerebrospinal fluid of MS is only rarely seen in NMO, (4) NMO may show brain lesions, although they are different from characteristic MS lesions. However, the patients during an early stage of NMO or those who have been actively treated may not show the characteristic clinical profile of NMO, and could be misdiagnosed. In this regard, a recent discovery of the specific serological marker of NMO (NMO-IgG or anti-AQP4 antibody) [Lennon *et al.* 2004; Lennon *et al.* 2005] has opened a new gate for diagnosis of NMO. The NMO-specific autoantibody was first identified in the sera from NMO as 'NMO-IgG' based on the ability to stain mouse CNS tissue. The target antigen of NMO-IgG was subsequently identified to be AQP4 [Lennon *et al.* 2005], which has led to establishment of assays that are more feasible and more sensitive than the original NMO-IgG assay [Paul *et al.* 2007; Tanaka *et al.* 2007; Takahashi *et al.* 2006].

Recent studies have shown that anti-AQP4 antibody or NMO-IgG can be detected in a large majority of NMO/OSMS patients, whereas most patients with conventional MS are anti-AQP4 negative [Paul *et al.* 2007; Tanaka *et al.* 2007; Nakashima *et al.* 2006]. Although, it has been argued whether NMO and MS represent distinct entities or not [Weinshenker *et al.* 2006; Kikuchi and Fukazaw, 2005], discovery of anti-AQP4 antibody has obviously strengthened the idea that typical NMO cases are distinct from MS in the pathogenesis. Furthermore, pathological analysis has recently demonstrated a remarkable loss of AQP4 [Misu *et al.* 2007; Roemer *et al.* 2007] along with concomitant absence of glial fibrillary acidic protein, a marker of astrocytes [Misu *et al.* 2007] in the lesions of NMO but not of MS. Although primary targets in MS are thought to be myelin and myelin-forming oligodendrocytes, the results of pathological studies suggest that astrocytes could be attacked by antibodies against AQP4 in NMO, further highlighting the differences between NMO and MS.

As mentioned above, patients predominantly manifesting optic nerve and spinal cord signs have been traditionally diagnosed as OSMS in Japan. A recent analysis showed that a majority of the OSMS patients are anti-AQP4 antibody positive and accompany the LESL, implying that most cases of OSMS could be diagnosed as NMO. However, some of the patients exhibited neither aniti-AQP4 nor LESL [Tanaka *et al.* 2007]. It is possible that these patients may

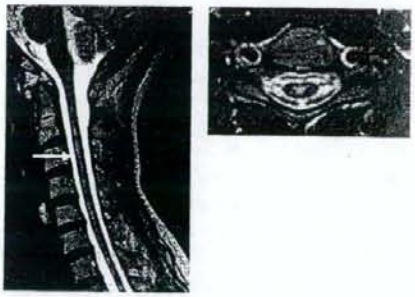

Figure 1. Longitudinally extensive spinal cord lesion (LESL) in a case of NMO T2-weighted cervical MRI demonstrates an extension of T2 high density involving central gray matter, which is characteristic of LESL associated with NMO.

Table 1. Brief history on NMO research.

Report	Year	Author
A report on a possible case with NMO	(1870)	Allbutto
A first case report on definitive NMO	(1894)	Devic
Proposal of a first diagnostic criteria	(1999)	Wingerchuk *et al.*
Discovery of NMO-IgG	(2004)	Lennon *et al.*
Identification of as a target of NMO-IgG	(2005)	Lennon *et al.*
Development of immunofluorescence assay for anti-AQP4 antibodies	(2006)	Takahashi *et al.*
Proposal of revised diagnostic criteria	(2006)	Wingerchuk *et al.*
Demonstration of AQP4 loss in NMO lesions	(2007)	Roemer *et al.*; Misu *et al.*

AQP4, aquaporin 4; NMO, neuromyelitis optica

belong to the category of MS, although the distribution of lesions resembles that of NMO.

Previously, presence of brain lesions and symptoms was an exclusion criterion for NMO. However, the revised diagnostic criteria allow diagnosis of NMO for patients who have brain lesions, provided that the MRI findings do not meet the diagnostic criteria for MS [Wingerchuk *et al.* 2006]. However, Matsuoka *et al.* reported on the presence of NMO patients, who have multiple juxtacortical or periventricular ovoid lesions in the brain, which is characteristic of MS, but not of NMO [Matsuoka *et al.* 2007]. Although this information may be used to argue against the distinction between MS and NMO, we would rather interpret that the patients might have both MS and NMO simultaneously. This possibility needs to be verified rigorously in future studies.

As such, discovery of anti-AQP4 antibody has greatly influenced on the understanding the pathogenesis of NMO. However, it remains unclear whether anti-AQP4 truly plays a role in the formation of destructive lesions in the optic nerve and spinal cord, although the selective loss of AQP4 in the NMO lesions indicate the pathogenic role of anti-AQP4 antibody. A number of investigators are trying to reproduce the pathology of NMO in rodents by passively transferring anti-AQP4 antibody. However, the results have not been published yet. Currently, it remains possible that pathogenic autoantibody in NMO may target CNS antigens other than AQP4.

Cerebrospinal fluid findings in NMO

Cerebrospinal fluid (CSF) examination could also be useful for distinguishing NMO from MS. For instance, presence of prominent CSF pleocytosis ($>50 \times 10^6$ WBC/L) during acute phase could be regarded as supporting diagnosis of NMO but not of MS [Wingerchuk *et al.* 1999]. It is also of note that OBs could be detected more frequently in MS than in NMO [Bergamaschi *et al.* 2004; Misu *et al.* 2002]. Misu *et al.* previously reported that OBs are negative in the Japanese OSMS patients who have no brain lesions on MRI [Misu *et al.* 2002]. However, Bergamaschi *et al.* have recently reported that presence of OBs could be demonstrated in 27% of NMO, when CSF samples were examined repeatedly [Bergamaschi *et al.* 2004]. Notably, the authors pointed out that OBs could be continuously detected during the course of MS, whereas appearance of OBs appears to be temporary in NMO, indicating the importance of repeated CSF examination to distinguish NMO from MS. Very recently, Jarius *et al.* have reported that a polyspecific humoral response against measles, rubella, and varicella zoster virus (MRZ) was positive in 37 out of 42 CSF samples from MS, but was detected only in one out of 20 samples from NMO. They suggest that assessment of the MRZ reaction in the CSF could also help in distinguishing MS and NMO [Jarius *et al.* 2008]. Taken together, these results indicate that a combination of CSF and serum studies may further improve diagnostic certainty.

Activation of IL-17/IL-8 axis in NMO

Besides an elevation of anti-AQP4, recent work has shown that IL-17 and IL-8 are specifically increased in the CSF from NMO [Ishizu *et al.* 2005]. IL-17 is a proinflammatory cytokine mainly produced by activated T cells, whose role in allergy and autoimmune inflammation has been highlighted lately. IL-8 is a chemokine whose major role is to recruit neutrophils. Of note, IL-8 production from macrophages and epithelial cells is promoted by IL-17. Because neutrophil infiltration is dominant in the necrotic lesions of NMO [Ishizu *et al.* 2005], the authors have argued that intrathecal activation of IL-17/IL-8 axis may uniquely contribute to the formation of destructive lesions found in NMO. If this is the case, an important question should be directed to the relationship between the IL-17/IL-8 axis and B cell immunity associated with an elevation of anti-AQP4 antibody. Though very little was known about the relationship between IL-17 and B cells, it has recently been reported that IL-17-producing T cells, namely Th17 cells [Bettelli *et al.* 2007; Steinman, 2007], would promote spontaneous formation of a germinal center and augment production of pathogenic autoantibodies in a model of systemic autoimmune disease [Hsu *et al.* 2008]. In the next section, we discuss on our hypothetical model in which the Th17 cell/B cell interaction plays a role in the pathogenesis of NMO.

Th17 cell biology and pathogenesis of NMO

Th17 cells are a novel helper T cell subset distinct from Th1 or Th2. Because it has been shown that Th17 cells play a decisive role in a variety of inflammatory processes, the biology

of Th17 cells is currently the subject of broad interest [Bettelli *et al.* 2007; Steinman 2007]. Before Th17 cells were identified, studies had emphasized the role of Th1 cells that produce interferon-γ in the pathogenesis of MS and its animal model experimental autoimmune encephalomyelitis (EAE). However, it now becomes clear that Th17 cells are crucial in the induction of EAE, and lymphocytes infiltrating the brain of MS would contain Th17 cells [Tzartos *et al.* 2008]. Although the pathogenic role of Th17 cells is sometimes being overemphasized, involvement of Th1 cells has been confirmed in various inflammatory pathologies. Interestingly, Th1 cells and Th17 cells express different sets of chemokine receptors [Sato *et al.* 2007], indicating that they might be recruited to different types of inflammatory lesions or to different anatomical sites.

Differentiation of rodent Th17 cells depends on IL-6 and transforming growth factor (TGF)-β [Bettelli *et al.* 2007] whereas human Th17 cells appear to be induced in the presence of IL-6 and IL-1β [Acosta-Rodriguez *et al.* 2007]. IL-23 is required for the expansion and maintenance of Th17 cells. As such IL-6 and IL-23 are now thought to be key cytokines in the generation of pathogenic Th17 cells.

The relation between Th17 cells and production of anti-AQP4 antibody is still not clear but could be speculated on the results of animal experiments. It is noteworthy that IL-17 produced by Th17 cells has recently been found to promote the germinal center formation in a spontaneous autoimmune disease model by altering the B cell chemotactic response, which leads to a massive production of pathogenic autoantibody [Hsu *et al.* 2008]. In contrast, blocking IL-17 signaling was inhibitory to the production of autoantibody and prevented the development of the autoimmune disease. These results indicate that Th17 cells would contribute to augmenting B cell autoimmunity through a mechanism distinct from its proinflammatory action. Notably, presence of a germinal center-like structure was demonstrated in the subarachnoid space of a rodent NMO model, which has been created by introducing genes for both T cell receptor (TCR) and B cell receptor for myelin oligodendrocytes glycoprotein (MOG) [Bettelli *et al.* 2006; Krishnamoorthy *et al.* 2006]. The mice spontaneously develop optic neuritis and myelitis. Furthermore, it is thought that collaboration of T cells (Th17) and B cells play a critical role in shaping the unique lesion distribution in this mouse model. If human NMO also involves a Th17 cell/B cell interaction, cytokines, chemokines and their receptors that play a role in Th17 cell-dependent production of pathogenic autoantibody could be potential therapeutic targets in NMO. The hypothetical model will be verified in a future study.

Interferon-β and NMO

Although a small preliminary report suggests the efficacy of interferon-β on OSMS [Saida *et al.* 2005], another study does not recommend its use for NMO in comparison with immunosuppressive agents [Papeix *et al.* 2007]. The most prominent and common side effects of interferon are a flu-like syndrome of fever, headache, myalgia, arthralgia, and general malaise. Furthermore, there are several case reports in Japan documenting a worsening of NMO [Warabi *et al.* 2007] or development of large brain lesions in NMO patients after starting interferon-β [Shimizu *et al.* 2008].

Although the clinical reports need to be carefully analyzed before making a conclusion, some cautions should be made upon the fact that type I interferon (including interferon-α and $-\beta$) would worsen or trigger the development of some antibody-mediated autoimmune diseases. For example, therapeutic use of type I interferon for cancer and hepatitis has been shown to cause exacerbation of SLE, thyroiditis, diabetes, psoriasis, rheumatoid arthritis, autoimmune hemolytic anemia, and myasthenia gravis [Baccala, *et al.* 2005; Theofilopoulos *et al.* 2005; Gota and Calabrise 2003; Stewart, 2003]. Among these, SLE and type I interferon has been causally linked following intensive analysis [Banchereau and Pascual, 2006; Pascual *et al.* 2006]. Early studies reported increased serum levels of IFN-α in lupus patients, which correlate with disease activity [Kim *et al.* 1987l; Ytterberg and Schnitzer, 1982]. More recently, microarray studies have identified increased expression of interferon-α- and interferon-γ-induced genes in peripheral blood lymphocytes of SLE patients in correlation with disease severity [Bennett *et al.* 2003; Baechler *et al.* 2003; Crow *et al.* 2003; Han *et al.* 2003]. Consistently, interferon-α was recently identified as the serum factor in SLE that could induce differentiation of dendritic cells with efficacious

antigen-presenting ability [Blanco *et al.* 2001]. Type I interferon might also contribute to immune complex formation in SLE by directly activating B cells [Le bon *et al.* 2001]. These results highlight the augmenting effect of type I interferon on antibody-mediated autoimmunity, which differs greatly from that of MS.

It is also of note that interferon-β shows a potential to induce IL-6 *in vitro* [Satoh *et al.* 2006] and *in vivo* [Nakatsuji *et al.* 2006]. IL-6 is a key cytokine involved in the induction of Th17 cells as well as growth and differentiation of B cells. Satoh *et al.* examined the gene expression profile of peripheral blood lymphocytes after culture with interferon-β and found a number of inflammatory cytokines including IL-6 are upregulated. Nakatsuji *et al.* has shown that the level of serum IL-6 after injection of interferon-β would correlate with side effects such as headache in the patients with MS, but ironically also predict the efficacy of interferon-β treatment in MS. Taken these together, injection of interferon-β could lead to induction of IL-6 at least transiently. From a theoretical point of view, one may argue that the IL-6-stimulatory property of interferon-β is not beneficial for treating NMO involving B cells and Th17 cells, both of which are responsive to IL-6. A systematic retrospective survey for interferon-β treated NMO patients will clarify if this concern is appropriate or not.

According to recent studies, abnormalities found in the brain MRI of NMO ranged from 10 to 50%. Asymptomatic brain lesions are now thought to be common in NMO, and symptomatic brain lesions do not exclude the diagnosis of NMO. Cabrera-Gómez *et al.* has reported that none of the brain MRI abnormalities in NMO were compatible with the criteria of MS brain lesions proposed by Barkhof *et al.* (1997) [Cabrera-Gómez *et al.* 2007]. As an extreme example, we show a patient with NMO, who developed a few large lesions in the brain white matter two months after starting interferon-β (Figure 2). A recent report by Shimizu *et al.* has also described the presence of similar NMO patients who developed large brain lesions after starting interferon-β [Shimizu *et al.* 2008]. The initial clinical and radiological features of our patient were consistent with NMO, and anti-AQP4 antibody was positive. This case suggests to us that a unique pattern of NMO lesion distribution could be transformed into another pattern of disease after undergoing

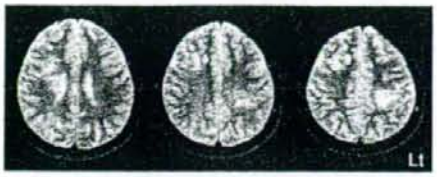

Figure 2. Development of large white matter lesions in a case of neuromyelitis optica (NMO) 2 months after starting interferon-β This young female patient was aquaporin 4 antibody-positive and showed a clinical and radiological picture characteristic of NMO. However, two months after starting interferon-β 1b treatment, she developed signs of brain hemispheres and MRI showed multiple large white matter lesions.

imunomodulation. We also speculate that interferon-β treatment might have triggered the unusual relapse in NMO.

Therapy of NMO in practice

At present, very little information is available that helps physicians and patients choose the best treatment for NMO. In general, treatment of acute exacerbation of NMO may start with intravenous corticosteroids (typically 1,000 mg of methylprednisolone for 3–5 consecutive days). Because the efficacy of plasma exchange was reported in NMO-IgG-positive patients with NMO [Watanabe *et al.* 2007a], plasmapheresis could be considered if clinical improvement is not satisfactory. However, effects of plasmapheresis are not consistent, and anti-AQP4 antibody could rise rapidly after plasmapheresis (Figure 3). To prevent the rebound of pathogenic antibody titers after plasma exchange, a combination therapy with immunosuppressive agents may be needed in some cases. Figure 3 demonstrates the clinical course of representative patients who were treated with plasmapheresis (plasma exchange or immunoadsorption (IA)). In the first case (Figure 3(a)), intravenous methylprednisolone (IVMP) treatment was found to reduce anti-AQP4 antibody titers in the serum, which was accompanied with some clinical improvement. However, as residual symptoms were not tolerable, plasma exchange was subsequently applied, which led to further recovery and disappearance of anti-AQP4 antibody. In the second case (Figure 3(b)), IVMP treatment was followed by plasmapheresis by using IA. We found that the first course of the IVMP plus IA tended to increase the titers of

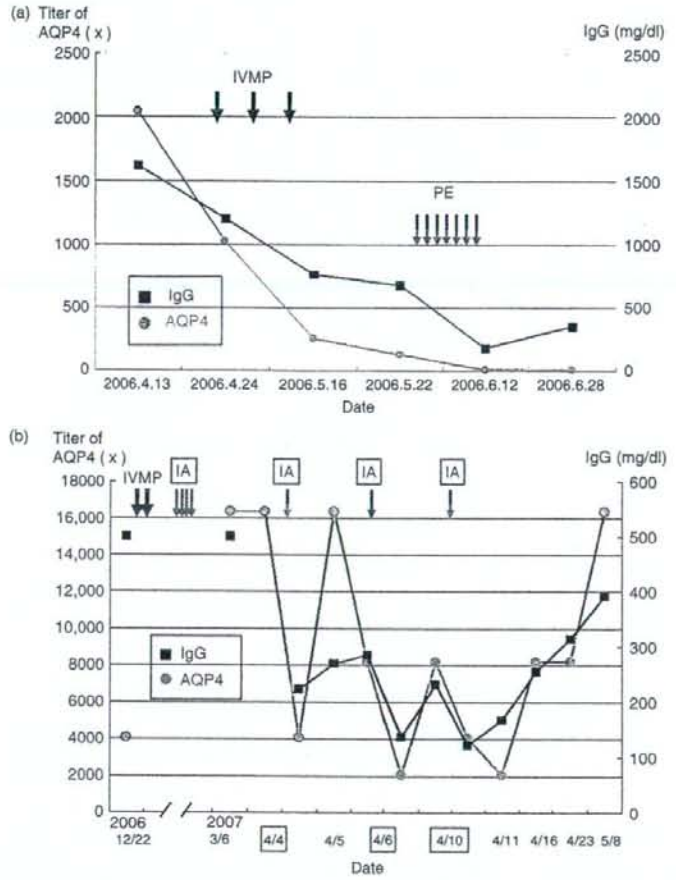

Figure 3. Treatment of NMO with plasmapheresis: representative cases (a) This 36-year-old female developed dysesthesia of the right leg and a constrictive band sensation in the chest region. A few days later, she experienced high fever, the loss of visual perception, progressive muscle weakness, and severe disturbance of sensation in all the limbs. She could not stand and suffered from neurogenic bladder. Treatment was initiated by the administration of 1000 mg/day of methylprednisolone (IVMP) for three consecutive days; this was followed by plasma exchange (PE) therapy which was conducted seven times over a two-week-period. The treatment was judged successful by clinical improvement as well as reduction of anti-aquaporin 4 (AQP4) antibody. (b) This 54-year-old female became completely paraplegic and was confined to bed after the development of thoracic transverse myelitis in December 2006. Although IVMP (1000 mg/day for five days followed by 500 mg/day for three days) and immunoadsorption (IA) therapies (four times) were applied, anti-AQP4 titers were somewhat elevated. So we checked the anti-AQP4 titer and total IgG before and after each of successive IA sessions. IA effectively removed the antibody and reduced the IgG amount after every IA session. But the titer and IgG returned rapidly. The anti-AQP4 antibody exhibits a higher rate of return to the basal level than that of the serum IgG. On evaluation on one month after the last IA, the patient's clinical improvement was very limited, and the anti-AQP4 antibody titer returned to the level of before starting the treatment.

anti-AQP4 antibody eleven weeks after starting the treatment. Subsequently, we measured the antibody titers and amount of serum IgG before and after each successive IA treatment. On each occasion, IA effectively removed the antibody and reduced the IgG amount. However, anti-AQP4 as well as total immunoglobulins recovered very quickly and returned to the pre-treatment level one month after the last IA. We attempted to add an immunosuppressive

drug, but the patient could not tolerate the side effects. The unsatisfactory result indicates that the primary target of therapy should be plasma cells producing pathogenic autoantibody.

To control the production of antibody, azathioprine could be used during the remission phase of NMO, often in combination with oral prednisone. Mandler *et al.* treated seven patients with newly diagnosed NMO with prednisone and azathioprine for 18 months. They found that relapses were prevented completely for more than 18 months and the patients improved significantly in the Expanded Disability Status Scale score [Mandler *et al.* 1998]. Figure 4 shows the clinical course of an anti-AQP4 antibody positive NMO patient being treated in our clinic. This NMO patient was in a state of remission for almost four years after two clinical attacks. However, she suddenly developed optic neuritis and myelitis at 57 years of age, and then interferon-β 1b therapy was introduced. The patient did not respond to the therapy, and clinical activity seemed to be even exacerbated. Because of frequent relapses, azathioprine (100 mg/day) was prescribed in addition. The patient then entered a state of remission, which was maintained even after stopping interferon-β. This interesting case indicates the efficacy of azathioprine in NMO.

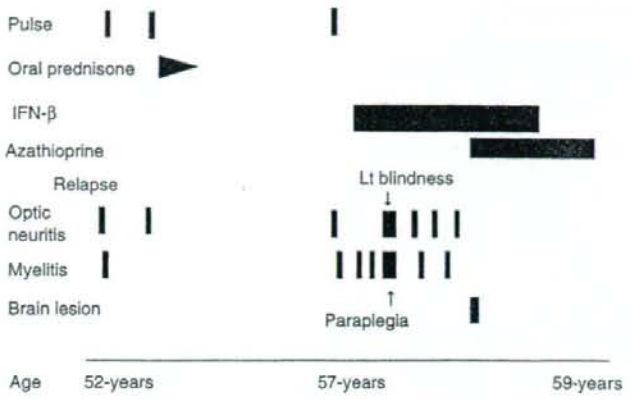

Figure 4. A patient with NMO who did not respond to interferon-β (IFN-β) but to azathioprine. Interferon-β was introduced to this female patient with NMO, as the patient's condition became active. However, there was no noticeable clinical benefit. After adding azathioprine, the patient entered a good remission state without any signs of relapses. Subsequently, we have withdrawn interferon-β, and the remission state is still continuing.

Recently, a retrospective investigation revealed that low-dose corticosteroids might reduce the rate of relapses in NMO [Watanabe *et al.* 2007b]. In some NMO patients, monthly intravenous infusion of immunoglobulin was reported to be effective [Bakker and Metz 2004]. Intravenous infusions of mitoxantrone hydrochloride (12 mg/m^2, monthly for six months followed by three additional treatments every three months) appeared to reduce relapses [Weinstock-Guttman *et al.* 2006]. As mitoxantrone would very potently suppress B-cell immunity directly or through a macrophage-mediated mechanism [Fidler *et al.* 1986], its efficacy in NMO is not unexpected. An open-label study of rituximab (a monoclonal antibody specific for CD20$^+$ B cells) showed an effective outcome for NMO [Cree *et al.* 2005]. Rituximab is an attractive treatment option for NMO because of its selective action against B cells. However, the potential risk and side effects should be taken into consideration. As an alternative therapeutic option, a single case report showed the efficacy of mycophenolate mofetil (2 g/day), which controls T cell-dependent antibody responses through purine synthesis inhibition [Falcini *et al.* 2006]. There is also a case report suggesting efficacy of glatiramer acetate on NMO [Bergamaschi *et al.* 2003].

Concluding remark

NMO is an autoimmune CNS disease characterized by the presence of anti-AQP4 antibody. According to the latest criteria for diagnosis, typical cases of NMO could be easily differentiated from MS by measuring anti-AQP4 antibody and examining the presence of LESL by spinal MRI. However, patients who have been treated with interferon-β or immunosuppressive drugs may show an atypical presentation, such as association of large brain lesions or clinical presentation of NMO without accompanying detectable anti-AQP4 antibody titers. Moreover, if the available anti-AQP4 assay is not sensitive enough, it might be hard to make a conclusive diagnosis of NMO. Interestingly, transgenic mice bearing MOG-specific T cell and B cell receptor are reported to exhibit NMO-like pathology, in which collaboration between T cells and B cells is critical [Bettelli *et al.* 2006; Krishnamoorthy *et al.* 2006]. By contrast, it remains unclear whether anti-AQP4 antibody may be truly pathogenic. It is rather promising to target B cells by a

monoclonal antibody like rituximab or block the T cell-B cell interaction by available drugs. An increase of IL-17 in the CSF also tempts us to consider therapy that modulates IL-6 or IL-23 signaling, which is involved in the generation and maintenance of Th17 cells. Because of recent advances in research, it may not take so long to establish a reasonable and more efficacious protocol for treatment of NMO.

Acknowledgment

We thank Dr Toshiyuki Takahashi at Tohoku University for measuring anti-AQP4 antibody levels.

Conflict of interest statement

None declared.

References

Acosta-Rodriguez, E., Napolitani, G., Lanzavecchia, A. and Sallusto, F. (2007) Interleukin 1beta and 6 but not transforming growth factor-beta are essential for the differentiation of interleukin 17-producing human T helper cells. *Nat Immunol* 8: 942–949.

Allbutt, T. (1870) On the ophthalmoscopic signs of spinal disease. *Lancet* 1: 76–78.

Baccala, R., Kono, D.H. and Theofilopoulos, A.N. (2005) Interferons as pathogenic effectors in autoimmunity. *Immunol Rev* 204: 9–26.

Baechler, E.C., Batliwalla, F.M., Karypis, G., Gaffney, P.M., Ortmann, W.A., Espe, K.J. *et al.* (2003) Inerferon-inducible gene expression signature in peripheral blood cells of patients with severe lupus. *Proc Natl Acad Sci USA* 100: 2610–2615.

Bakker, J. and Metz, L. (2004) Devic's neuromyelitis optica treated with intravenous gamma globulin (IVIG). *Can J Neurol Sci* 31: 265–267.

Banchereau, J. and Pascual, V. (2006) Type I interferon in systemic lupus erythematosus and other autoimmune diseases. *Immunity* 25: 383–392.

Barkhof, F., Filippi, M., Miller, D.H., Sheltens, P., Campi, A., Polman, C.H. *et al.* (1997) Comparison of MRI criteria at first presentation to predict conversion to clinically definite multiple sclerosis. *Brain* 120: 2059–2069.

Bennett, L., Palucka, A.K., Arce, E., Cantrell, V., Borvak, J., Banchereau, J. and Pascual, V. (2003) Interferon and granulopoiesis signatures in systemic lupus erythematosus blood. *J Exp Med* 197: 711–723.

Bergamaschi, R., Uggetti, C., Tonietti, S., Egitto, M.G. and Cosi, V. (2003) A case of relapsing neuromyelitis optica treated with glatiramer acetate. *J Neurol* 250: 359–361.

Bergamaschi, R., Tonietti, S., Franciotta, D., Candeloro, E., Tavazzi, E., Piccolo, G. *et al.* (2004) Oligoclonal bands in Devic's neuromyelitis optica and multiple sclerosis: differences in repeated cerebrospinal fluid examinations. *Mult Scler* 10: 2–4.

Bettelli, E., Baeten, D., Jäger, A., Sobel, R.A. and Kuchroo, V.K. (2006) Myelin oligodendrocyte glycoprotein-specific T and B cells cooperate to induce a Devic-like disease in mice. *J Clin Invest* 116: 2393–2402.

Bettelli, E., Korn, T. and Kuchroo, V.K. (2007) Th17: the third member of the effector T cell trilogy. *Curr Opin Immunol* 19: 652–657.

Blanco, P., Palucka, A.K., Gill, M., Pascual, V. and Banchereau, J. (2001) Induction of dendritic cell differentiation by IFN-α in systemic lupus erythematosus. *Science* 294: 1540–1543.

Cabrera-Gómez, J.A., Quevedo-Sotolongo, L., Gonzalez-Quevedo, A., Lima, S., Real-Gonzalez, Y., Cristofol-Corominas, M. *et al.* (2007) Brain magnetic resonance imaging findings in relapsing neuromyelitis optica. *Mult Scler* 13: 186–192.

Cree, B.A., Lamb, S., Morgan, K., Chen, A., Waubant, E. and Genain, C. (2005) An open label study of the effects of rituximab in neuromyelitis optica. *Neurology* 64: 1270–1272.

Crow, M.K., Kirou, K.A. and Wohlgemuth, J. (2003) Microarray analysis of interferon-regulated genes in SLE. *Autoimmunity* 36: 481–490.

Devic, E. (1894) Myelite subaiguë compliquée de névrite optique. *Bull Med* 8: 1033–1034.

Falcini, F., Trapani, S., Ricci, L., Resti, M., Simonini, G. and de Martino, M. (2006) Sustained improvement of a girl affected with Devic's disease over 2 years of mycophenolate mofetil treatment. *Rheumatology (Oxford)* 45: 913–915.

Fidler, J.M., DeJoy, S.Q. and Gibbons, J.J. (1986) Selective immunomodulation by the antineoplastic agent mitoxantrone. I. Suppression of B lymphocyte function. *J Immunol* 15;137: 727–732.

Gota, C. and Calabrese, L. (2003) Induction of clinical autoimmune disease by therapeutic interferon-α. *Autoimmunity* 36: 511–518.

Han, G.M., Chen, S.L., Shen, N., Ye, S., Bao, C.K. and Gu, Y.Y. (2003) Analysis of gene expression profiles in human systemic lupus erythematosus using oligonucleotide microarray. *Genes Immun* 4: 177–186.

Hsu, H.-C., Yang, P., Wang, J., Wu, Q., Myers, R., Chen, J. *et al.* (2008) Interleukin 17-producing T helper cells and interleukin 17 orchestrate autoreactive germinal center development in autoimmune BXD2 mice. *Nature Immunol* 9: 166–175.

Ishizu, T., Osoegawa, M., Mei, F.J., Kikuchi, H., Tanaka, M., Takakura, Y. *et al.* (2005) Intrathecal

activation of the IL-17/IL-8 axis in opticospinal multiple sclerosis. *Brain* 128(Pt 5): 988–1002.

Jacob, A., Matiello, M., Wingerchuk, D.M., Lucchinetti, C.F., Pittock, S.J. and Weinshenker, B.G. (2007) Neuromyelitis optica: changing concepts. *J Neuroimmunol* 187: 126–138.

Jarius, S., Franciotta, D., Bergamaschi, R., Rauer, S., Wandinger, K.P., Petereit, H.F. *et al.* (2008) Polyspecific, antiviral immune response distinguishes multiple sclerosis and neuromyelitis optica. *J Neurol Neurosurg Psychiatry* epub February 12.

Kikuchi, S. and Fukazawa, T. (2005) OSMS is NMO, but not MS: confirmed by NMO-IgG? *Lancet Neurol* 4: 594–595.

Kim, T., Kanayama, Y., Negoro, N., Okamura, M., Takeda, T. and Inoue, T. (1987) Serum levels of interferons in patients with systemic lupus erythematosus. *Clin Exp Immunol* 70: 562–569.

Krishnamoorthy, G., Lassmann, H., Wekerle, H. and Holz, A. (2006) Spontaneous opticospinal encephalomyelitis in a double-transgenic mouse model of autoimmune T cell/B cell cooperation. *J Clin Invest* 116: 2385–2392.

Le bon, A., Schiavoni, G., D'Agostino, G., Gresser, I., Belardelli, F. and Tough, D.F. (2001) Type I interferons potently enhance humoral immunity and can promote isotype switching by stimulating dendritic cells in vivo. *Immunity* 14: 461–470.

Lennon, V.A., Wingerchuk, D.M., Kryzer, T.J., Pittock, S.J., Lucchinetti, C.F., Fujihara, K. *et al.* (2004) A serum autoantibody marker of neuromyelitis optica: distinction from multiple sclerosis. *Lancet* 364: 2106–2012.

Lennon, V.A., Kryzer, T.J., Pittock, S.J., Verkman, A.S. and Hinson, S.R. (2005) IgG marker of optic-spinal multiple sclerosis binds to the aquaporin-4 channel. *J Exp Med* 202: 473–477.

Mandler, R.N., Ahmed, W. and Dencoff, J.E. (1998) Devic's neuromyelitis optica: a prospective study of seven patients treated with prednisone and azathioprine. *Neurology* 51: 1219–1220.

Matiello, M., Jacob, A., Wingerchuk, D.M. and Weinshenker, B.G. (2007) Neuromyelitis optica. *Curr Opin Neurol* 20: 255–260.

Matsuoka, T., Matsushita, T., Kawano, Y., Osoegawa, M., Ochi, H., Ishizu, T. *et al.* (2007) Heterogeneity of aquaporin-4 autoimmunity and spinal cord lesions in multiple sclerosis in Japanese. *Brain* 130: 1206–1223.

Misu, T., Fujihara, K., Nakashima, I., Miyazawa, I., Okita, N., Takase, S. *et al.* (2002) Pure optic-spinal form of multiple sclerosis in Japan. *Brain* 125: 2460–2468.

Misu, T., Fujihara, K., Kakita, A., Konno, H., Nakamura, M., Watanabe, S. *et al.* (2007) Loss of aquaporin 4 in lesions of neuromyelitis optica: distinction from multiple sclerosis. *Brain* 130: 1224–1234.

Nakashima, I., Fujihara, K., Miyazawa, I., Misu, T., Narikawa, K., Nakamura, M. *et al.* (2006) Clinical and MRI features of Japanese patients with multiple sclerosis positive for NMO-IgG. *J Neurol Neurosurg Psychiatry* 77: 1073–1075.

Nakatsuji, Y., Nakano, M., Moriya, M., Kishigami, H., Tatsumi, C., Tada, S. *et al.* (2006) Beneficial effect of interferon-β treatment in patients with multiple sclerosis is associated with transient increase in serum IL-6 level in response to interferon-β injection. *Cytokine* 36: 69–74.

Papeix, C., Vidal, J.S., de Seze, J., Pierrot-Deseilligny, C., Tourbah, A., Stankoff, B. *et al.* (2007) Immunosuppressive therapy is more effective than interferon in neuromyelitis optica. *Mult Scler* 13: 256–259.

Paul, F., Jarius, S., Aktas, O., Bluthne, R.M., Baue, R.O., Appelhan, H. *et al.* (2007) Autoantibody to aquaporin 4 in the diagnosis of neuromyelitis optica. *PLoS Med* 4: e133.

Pascual, V., Farkas, L. and Banchereau, J. (2006) Systemic lupus erythematosus: all roads lead to type I interferons. *Curr Opin Immunol* 18: 676–682.

Roemer, S.F., Parisi, J.E., Lennon, V.A., Benarroch, E.E., Lassmann, H., Bruck, W. *et al.* (2007) Pattern-specific loss of aquaporin-4 immunoreactivity distinguishes neuromyelitis optica from multiple sclerosis. *Brain* 130: 1194–1205.

Saida, T., Tashiro, K., Itoyama, Y., Sato, T., Ohashi, Y., Zhao, Z. *et al.* (2005) Interferon beta-1b is effective in Japanese RRMS patients: a randomized multicenter study. *Neurology* 64: 621–630.

Sato, W., Aranami, T. and Yamamura, T. (2007) Cutting Edge. Human Th17 cells are identified as bearing $CCR2^{+}CCR5^{-}$ phenotype. *J Immunol* 178: 7525–7529.

Satoh, J., Nanri, Y., Tabunoki, H. and Yamamura, T. (2006) Microarray analysis identifies a set of CXCR3 and CCR2 ligand chemokines as early IFNβ -responsive genes in peripheral blood lymphocytes in vitro: an implication for IFNβ -related adverse effects in multiple sclerosis. *BMC Neurol* 6: 18.

Shimizu, Y., Yokoyama, K., Misu, T., Takahashi, T., Fujihara, K., Itoyama, Y., Iwata, M. *et al.* (2008) Development of extensive brain lesions following interferon beta therapy in relapsing Neuromyelitis optica and longitudinally extensive myelitis. *J Neurol* 255: 305–307.

Steinman, L. (2007) A brief history of T_H17, the first major revision in the T_H1/T_H2 hypothesis of T cell-mediated tissue damage. *Nat Med* 13: 139–145.

Stewart, T.A. (2003) Neutralizing interferon alpha as a therapeutic approach to autoimmune diseases. *Cytokine Growth Factor Rev* 14: 139–154.

Takahashi, T., Fujihara, K., Nakashima, I., Misu, T., Miyazawa, I., Nakamura, M. *et al.* (2006) Establishment of a new sensitive assay for anti-human aquaporin-4 antibody in neuromyelitis optica. *Tohoku J Exp Med* 210: 307–313.

Tanaka, K., Tani, T., Tanaka, M., Saida, T., Idezuka, J., Yamazaki, M. *et al.* (2007) Anti-aquaporin 4 antibody in selected Japanese multiple sclerosis patients with long spinal cord lesions. *Mult Scler* 13: 850–855.

Theofilopoulos, A.N., Baccala, R., Beutler, B. and Kono, D.H. (2005) Type I Interfesons (α/β) in immunity and autoimmunity. *Annu Rev Immunol* 23: 307–336.

Tsartos, J.S. *et al.* (2008) Interleukin-17 production in central nervous system-infiltrating T cells and glial cells is associated with active disease in multiple sclerosis. *Am J Pathol* 172: 146–155.

Warabi, Y., Matsumoto, Y. and Hayashi, H. (2007) Interferon beta-1b exacerbates multiple sclerosis with severe optic nerve and spinal cord demyelination. *J Neurol Sci* 252: 57–61.

Watanabe, S., Nakashima, I., Misu, T., Miyazawa, I., Shiga, Y., Fujihara, K. *et al.* (2007a) Therapeutic efficacy of plasma exchange in NMO-IgG-positive patients with neuromyelitis optica. *Mult Scler* 13: 128–132.

Watanabe, S., Misu, T., Miyazawa, I., Nakashima, I., Shiga, Y., Fujihara, K. *et al.* (2007b) Low-dose corticosteroids reduce relapses in neuromyelitis optica: a retrospective analysis. *Mult Scler* 13: 968–974.

Weinshenker, B.G., Wingerchuk, D.M., Nakashima, I., Fujihara, K. and Lennon, V.A. (2006) OSMS is NMO, but not MS: proven clinically and pathologically. *Lancet Neurol* 5: 110–111.

Weinstock-Guttman, B., Ramanathan, M., Lincoff, N., Napoli, S.Q., Sharma, J., Feichter, J. *et al.* (2006) Study of mitoxantrone for the treatment of recurrent neuromyelitis optica (Devic disease). *Arch Neurol* 63: 957–963.

Wingerchuk, D.M., Ramanathan, M., Lincoff, N., Napoli, S.Q., Sharma, J., Feichter, J. *et al.* (1999) The clinical course of neuromyelitis optica (Devic's syndrome). *Neurology* 53: 1107–1114.

Wingerchuk, D.M., Lennon, V.A., Pittock, S.J., Lucchinetti, C.F., Weinshenker, B.G. *et al.* (2006) Revised diagnostic criteria for neuromyelitis optica. *Neurology* 66: 1485–1489.

Wingerchuk, D.M., Lennon, V.A., Lucchinetti, C.F., Pittock, S.J., Weinshenker, B.G. *et al.* (2007) The spectrum of neuromyelitis optica. *Lancet Neurol* 6: 805–815.

Yttenberg, S.R. and Schnitzer, T.J. (1982) Serum interferon levels in patients with systemic lupus erythematosus. *Arthritis Rheum* 25: 401–406.

Acta Neuropathol (2008) 116:561–566
DOI 10.1007/s00401-008-0425-8

ORIGINAL PAPER

Plaque-type deposition of prion protein in the damaged white matter of sporadic Creutzfeldt-Jakob disease MM1 patients

Atsushi Kobayashi · Kunimasa Arima · Masafumi Ogawa · Miho Murata · Takahiro Fukuda · Tetsuyuki Kitamoto

Received: 29 July 2008 / Revised: 20 August 2008 / Accepted: 20 August 2008 / Published online: 28 August 2008

Abstract Plaque-type deposition of prion protein (PrP) in the brain has been extremely rare in sporadic Creutzfeldt-Jakob disease patients with methionine homozygosity at polymorphic codon 129 of the PrP gene and type 1 abnormal isoform of PrP (sCJD-MM1). Here we report three sCJD-MM1 patients who showed prominent PrP-positive amyloid plaques in the cerebral and cerebellar white matter. All three patients showed clinical courses of long duration (2 years ≤), particularly at the end-stage. The white matter of these patients was severely damaged because of the prolonged disease duration. Furthermore, Alzheimer's amyloid precursor protein, which accumulates within the axonal swellings under pathological conditions, co-accumulated with the PrP-amyloid plaques. These findings suggest that the axonal damage reflecting the prolonged disease duration causes the deposition of PrP-amyloid plaques in the white matter. The present study shows that PrP-amyloid plaques can occur in the white matter of sCJD-MM1 cases.

Keywords Creutzfeldt-Jakob disease · Prion protein · Amyloid plaque · White matter

A. Kobayashi · T. Kitamoto (✉)
Division of CJD Science and Technology,
Department of Prion Research,
Tohoku University Graduate School of Medicine,
2-1 Seiryo-machi, Aoba-ku, Sendai 980-8575, Japan
e-mail: kitamoto@mail.tains.tohoku.ac.jp

K. Arima
Department of Laboratory Medicine,
National Center of Neurology and Psychiatry Musashi Hospital,
4-1-1 Ogawa-higashi-machi, Kodaira 187-8511, Japan

M. Ogawa · M. Murata
Department of Neurology,
National Center of Neurology and Psychiatry Musashi Hospital,
4-1-1 Ogawa-higashi-machi, Kodaira 187-8511, Japan

T. Fukuda
Division of Neuropathology,
Department of Neuroscience, Research Center for Medical Sciences, The Jikei University School of Medicine,
3-25-8 Nishi-Shimbashi, Minato-ku 105-8461, Japan

Introduction

The clinicopathologic phenotypes of sporadic Creutzfeldt-Jakob disease (sCJD) correlate with the genotype [methionine (M) or valine (V)] at polymorphic codon 129 of the prion protein (PrP) gene and the type (type 1 or type 2) of abnormal isoform of PrP (PrP^{Sc}) in the brain [14–16]. Type 1 and type 2 PrP^{Sc} are distinguishable according to the size of the proteinase K-resistant core of PrP^{Sc} (PrP^{res}) (21 and 19 kDa, respectively), reflecting differences in the proteinase K-cleavage site (at residues 82 and 97, respectively) [14, 17]. Based on the genotype and the PrP^{Sc} type, sCJD can be classified into six groups (MM1, MM2, MV1, MV2, VV1 and VV2) [16].

Nearly 70% of sCJD cases are classified as MM1 [16]. sCJD-MM1 is characterized by a clinical course of short duration (mean duration: 3.9 months) and synaptic-type PrP deposition in the brain [16]. However, a small subpopulation of sCJD-MM1 shows long disease duration over several years [16]. The prolonged disease duration might be due to the younger age at onset [18], or to the intensive care of the patients [5], since a comprehensive study revealed no significant difference in the physicochemical properties of PrP^{Sc} between the sCJD-MM1 cases with short and long disease duration[2]. By contrast, the synaptic-type PrP deposition is a common feature of sCJD-MM1 cases. Plaque-type PrP deposition has been extremely rare in sCJD-MM1 cases [16].

Table 1 Summary of the clinical features

	Patient 1	Patient 2	Patient 3
Sex	Male	Male	Female
Age at onset (years)	69	63	71
Initial symptoms	Progressive dementia Fatigue	Progressive dementia	Progressive dementia Fatigue
Myoclonus (months)[a]	5	8	3
Akinetic mutism (months)[a]	7	12[b]	6
PSWC on EEG (months)[a]	5	–[c]	2
Duration (months)	38	24	24

[a] The duration until the appearance of myoclonus, akinetic mutism, or PSWC from onset

[b] The patient became bedridden 7 months after the initial symptoms

[c] Only a single EEG examination was performed 2 months after the initial symptoms. EEG revealed a short burst of delta waves and slowing of background activities

Here we report three sCJD-MM1 patients with prominent PrP-positive amyloid plaques in the cerebral and cerebellar white matter. All three patients showed clinical courses of long duration. Therefore, we discuss correlations among the long disease duration, white matter involvement, and PrP-amyloid plaques.

Patients and methods

Patients

The clinical features of the three patients are summarized in Table 1 and Fig. 1. The clinical signs at onset were complaint of fatigue and progressive dementia (memory loss, disorientation and miscalculation). Electroencephalogram (EEG) showed periodic sharp wave complex (PSWC) in patients 1 and 3. In patient 2, only a single EEG examination was performed 2 months after the initial symptoms, which revealed a short burst of delta waves and slowing of background activities. The patients became bedridden 5 months (patient 1), 7 months (patient 2), or 4 months (patient 3) after the initial symptoms, and then fell into akinetic mutism 7 months (patient 1), 12 months (patient 2), or 6 months (patient 3) after the onset. The total disease duration was 38 months (patient 1) or 24 months (patients 2 and 3). The past medical history was unremarkable with no neurological surgery, no exposure to iatrogenic CJD, and no brain trauma. There was no family history of similar disorders.

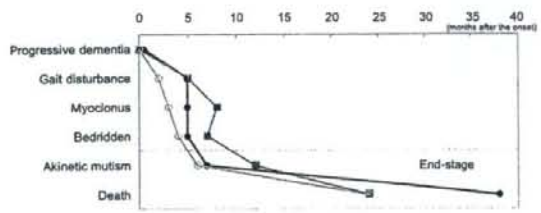

Fig. 1 The clinical courses of patient 1 (*filled circle*), patient 2 (*filled square*), and patient 3 (*open circle*). After the rapid exacerbation period, a prolonged end-stage followed

PrP gene analysis

Genomic DNA was extracted from peripheral blood leukocytes, and the coding region of the PrP gene was analyzed as previously described [7].

Western blot analysis

Brain tissues were obtained at autopsy after receiving informed consent for research use. The brains were immediately frozen or fixed in 10% buffered formalin. PrP^{Sc} was extracted from the frontal cortex with collagenase treatment as described [3] with modifications. Samples were subjected to 13.5% SDS-PAGE and western blotting as described [1]. The 3F4 monoclonal antibody (Signet Laboratories) was used as the primary antibody. Goat-anti-mouse immunoglobulin polyclonal antibody labeled with the peroxidase-conjugated dextran polymer, EnVision+ (DakoCytomation), was used as the secondary antibody.

Neuropathology

Formalin-fixed brains were treated with 99% formic acid for 1 h to inactivate the infectivity and were embedded in paraffin. Tissue sections were stained with hematoxylin and eosin (H&E) for routine neuropathological examination. For Congo red staining, tissue sections were incubated in a solution containing 1% Congo red and 50% ethanol for

30 min. After washing with a solution containing 50% ethanol and 1% sodium hydroxide, the sections were counterstained with hematoxylin. For the PrP immunohistochemistry, tissue sections were pretreated by hydrolytic autoclaving [6]. The #71 monoclonal antibody was used as the primary antibody [10, 19]. Anti-mouse EnVision+ was used as the secondary antibody. For the immunohistochemical detection of the Alzheimer's amyloid precursor protein (APP), tissue sections were pretreated by hydrated autoclaving with 10 mM EDTA pH 6.0 [11, 20]. The UT-18 polyclonal antibody was used as the primary antibody [21]. Anti-rabbit EnVision+ was used as the secondary antibody. The color was developed with diaminobenzidine for single immunostaining or with diaminobenzidine and cobalt chloride [12] for double staining. For double staining with Congo red, the color-developed immunostained sections were washed with water for 5 min and then stained with Congo red as described earlier. In this paper, we term PrP deposits clearly observed on H&E-stained sections and showing green birefringence on adjacent Congo red-stained sections as (amyloid) plaques. Focal PrP-immunolabelings are generically termed as plaque-type PrP deposits, which include amyloid plaques.

Results

PrP gene analysis

All three patients were homozygous for methionine at polymorphic codon 129 (129 M/M) and for glutamic acid at polymorphic codon 219 (219E/E) of the PrP gene. There was no mutation in the coding region of the PrP gene.

Western blot analysis

Western blot analysis of the brains after proteinase-K digestion revealed that the size of PrP^{res} was identical with type 1 PrP^{res} from a typical sCJD-MM1 case (Fig. 2). Type 2 PrP^{res} was not detected.

Neuropathology

The brains weighed 680 g (patient 1), 1,000 g (patient 2), or 840 g (patient 3). The cerebral cortex was very thin, and the white matter was atrophic. On microscopic examination, severe neuronal loss and marked astrocytosis were observed in the cerebral cortex, thalamus and cerebellar cortex (Fig. 3a). The basal ganglia, hippocampus and brainstem were relatively spared. The cerebral and cerebellar white matter showed severe degeneration with the infiltration of macrophages. In patients 1 and 2, many amyloid plaques were observed in the white matter of the

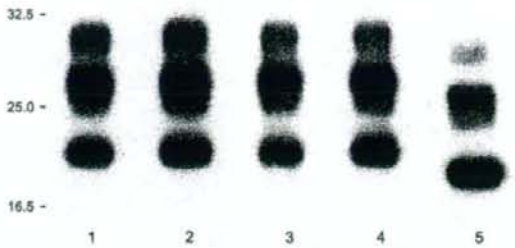

Fig. 2 Western blot analysis of PrP^{res} in the homogenates of the frontal cortex from patient 1 (*lane 2*), patient 2 (*lane 3*), or patient 3 (*lane 4*). The size and glycosylation pattern of PrP^{res} from the three patients were identical with type 1 PrP^{res} from a typical sCJD-MM1 case (*lane 1*), but different from type 2 PrP^{res} from a sCJD-MM2 case (*lane 5*)

cerebral cortex, parahippocampal gyrus, basal ganglia, thalamus, and cerebellar cortex (Fig. 3b). Congo red staining revealed that these amyloid plaques showed green birefringence under polarized light (Fig. 3c). Immunohistochemical analysis using anti-human PrP antibody #71 revealed numerous plaque-type PrP deposits in the white matter besides synaptic-type PrP deposition in the grey matter (Fig. 3d–f). PrP-positive plaques were prominent particularly in the parahipocampal gyrus and basal ganglia (Table 2). In patient 3, plaque-type PrP deposition in the white matter was restricted to within the parahippocampal gyrus.

To evaluate the extent of the axonal damage, we investigated the accumulation of APP in the white matter. APP accumulates within the axonal swellings of brain lesions such as those by infarction [13]. Therefore, we performed immunohistochemical analysis using anti-APP polyclonal antibody UT-18 [21]. In patients 1 and 2, there were many APP immunoreactivities in the white matter of the parahippocamupal gyrus and basal ganglia (Fig. 4a). The accumulation of APP was also observed in the white matter of the frontal and temporal cortex of patient 2. APP accumulation was not observed in the brain sections from patient 3 or typical sCJD-MM1 cases with short disease duration (data not shown). Thus, the intensity and distribution of APP immunoreactivities in the white matter correlated well with those of PrP-amyloid plaques. Furthermore, some of these APP immunoreactivities were enclosed in amyloid plaque-like structures (Fig. 4b). Double staining with APP immunohistochemistry and Congo red revealed the co-localization of APP and amyloid plaques (Fig. 4c). To examine the co-accumulation of APP and PrP, we performed immunohistochemical analysis of the serial sections using anti-APP or anti-PrP antibody. A significant portion of the APP immunoreactivities was co-localized with PrP-amyloid plaques in patients 1 and 2 (Fig. 4d, e).